Interactions between aluminium ions and acrylic acid–acrylamide copolymers in aqueous solution: 2. Phase separation

Ramine Rahbari and Jeanne François
Institut Charles Sadron, CRM, Université Louis Pasteur, 6 rue Boussingault, 67083 Strasbourg, France

(*Received 26 June 1987; accepted 5 November 1987*)

The stability of aqueous solutions of acrylic acid–acrylamide copolymers (with acrylate content τ varying from 0.3 to 27%) towards Al species has been investigated at different pH values. In our previous work, an electrostatic interaction model was proposed which predicted first that the polymer stability is at a minimum at pH 5 (due to the presence of Al polycations) and secondly that there is no interaction between polymer and Al at pH 7 (due to the presence of non-ionic $Al(OH)_3$ species). The second prediction is incorrect and phase diagrams were established at pH 5 as well as at pH 7, and allowed us to determine: (a) the critical concentration C_a^* of the Al (for which polymer precipitation occurs) as a function of polymer concentration and (b) the C_a^* dependence on τ. The fraction of precipitated polymer was evaluated using two techniques (potentiometric titration of the supernatant and carbon titration in the precipitated phase). This was compared, at low pH ($\leqslant 5$) with the calculated results of the electrostatic interaction model. An interesting result was the finding of gel formation at pH 5, for one of our polymer samples in the presence of Al.

(Keywords: acrylic acid–acrylamide copolymer; stability; gelation)

INTRODUCTION

In a recent work[1], we studied the interactions between partially hydrolysed polyacrylamide (HPAM) and different species of aluminium ions in aqueous solutions, using ^{27}Al n.m.r. spectroscopy. More precisely, this technique allowed us to determine the fraction of bound aluminium, which is found to be maximum for two pH values: 4.3 and 4.8. This result is in good agreement with the predictions of a simple model of electrostatic interactions, the first maximum corresponding to binding of Al^{3+} ions and the second one to that of polynuclear ions, $Al_{13}(OH)_{27}^{3+}$.

In fact, n.m.r. spectroscopy can only be used to determine the amount of ionic species of aluminium[2–7] in solution, and near pH 7, when the non-ionic $Al(OH)_3$ is preponderant, other techniques must be used to study the HPAM–Al interactions.

On the other hand, acrylic acid–acrylamide copolymers can be used in the tertiary oil recovery process as thickening agents[8–11], and the main problem of this application consists of the loss of viscosity and phase separation in the presence of metallic species.

The main purpose of this study is to establish the phase separation diagram as a function of copolymer composition, in the range of pH near neutrality ($5 < pH < 8$). Our investigations deal with the amount of precipitated polymer at phase separation, the change of viscosity and the aggregation state of the polymer.

EXPERIMENTAL

Samples

Five polymer samples have been used. Samples AD10, AD17, AD27 and AD37, supplied by Rhône-Poulenc, have been prepared by photo-copolymerization of acrylamide and sodium acrylate[12]. Their acrylate contents (τ), measured by potentiometry, elemental analysis and ^{13}C n.m.r., are 1.5, 7, 17 and 27% respectively[13]. The molecular weight M_w of the four samples is approximately 5×10^6. The last sample (PAM-NH) has been prepared in our laboratory by photopolymerization (γ-rays) ($\tau = 0.3\%$ and $M_w = 10^6$).

Preparation of the solutions

$AlCl_3$ solutions of given concentrations ($0 < C_a < 20$ ppm) were neutralized by addition of small volumes of NaOH solutions of concentration 10 times higher, the neutralization ratio ranging between 0 and 3. The neutralized solutions were slightly stirred and were used within one week.

The industrial polymer samples are sodium salts of acrylamide–acrylic acid copolymer. Their solutions at a given concentration are homogenized by slow stirring at room temperature for at least one day and the pH is adjusted by addition of 0.1 N HCl.

Except for the preparations for light scattering experiments, the following procedure was used for the mixed polymer–$AlCl_3$ solutions: in order to avoid inhomogeneities due to strong interactions between the two compounds, for a given composition C_p and C_a, the solutions were obtained by mixing two equal volumes of a polymer solution of concentration $2C_p$ and of an $AlCl_3$ solution of concentration $2C_a$, each of them being adjusted at the same pH.

Turbidimetry

The turbidity of the solutions was measured with a Shimadzu UV 240 spectrophotometer at 700 nm. *Figure 1*

0032–3861/88/050851–09$03.00

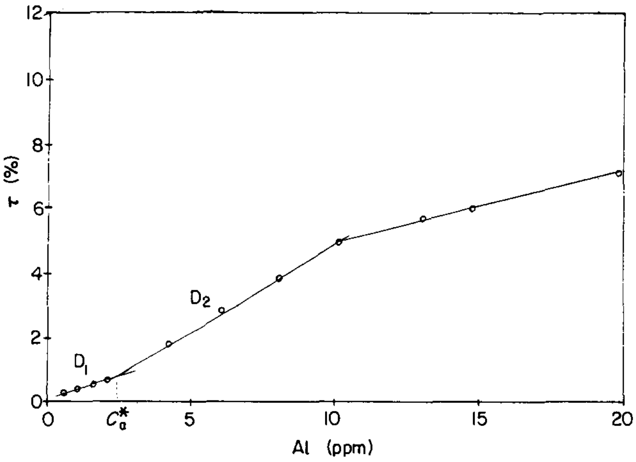

Figure 1 Example of turbidimetric curve for AD27 (250 ppm) at pH 5

shows a typical turbidity variation with Al content, at a given C_p. The critical concentration C_a^* corresponds to the abrupt turbidity change and is determined by linear regression on experimental points of straight lines D_1 and D_2. Above C_a^*, the system is considered to present phase separation.

Titration of the phases

The phase compositions have been measured either by potentiometric titration of the supernatant or by determination of the carbon content of the precipitated phase.

Potentiometric titration of the supernatant. The mixed polymer–$AlCl_3$ solutions were stirred for 2 h and were then filtered on 90 μm cellulose filters. The supernatant solutions were successively stirred with a large excess of anionic and cationic exchange resins in order to eliminate all the low-molecular-weight ionic species. The solution of acid copolymer was titrated by potentiometry by using a Metrohm 605 pH meter with a glass combined microelectrode. The polymer concentration was deduced from the equivalent volume of 0.01 N NaOH solution.

Carbon titration in precipitated phase. Some 400 cm^3 of mixed polymer–$AlCl_3$ solutions, at a given pH, were stirred and then filtered on glass filters of porosity higher than that of cellulose filters. The coacervate was dried and weighed and the carbon content was determined by elemental analysis. By assuming that the coacervate does not contain sodium, one can calculate from these two measurements the fraction of precipitated polymer and the content of Al in the coacervate.

Viscometry

The viscosity measurements were performed with a low-shear viscometer (Contraves LS30) equipped with the system 2T2T ($\Phi = 11$ mm, $L = 20$ mm, $e = 1$ mm) and thermostatted at 25°C. The measurements were carried out on filtered solutions for $C_a > C_a^*$.

In the case of unhydrolysed sample of relatively low molecular weight, viscosity measurements were made with an automatic capillary viscometer[14] of higher accuracy, the shear rate effect being negligible.

Light scattering

Light scattering experiments were made with a home-built apparatus[15] (wavelength = 6320 Å) for diffusion angle θ varying between 30° and 150°. We used the values of refractive index increment dn/dc obtained in a previous work[16].

For these measurements, we have tried another procedure than that previously described above: this method was based on a dialysis technique. One compartment of a high-volume (2×400 cm^3) dialysis cell contained a polymer solution at a given pH, previously filtered on Millipore (0.8 μm); and the second one was filled with an $AlCl_3$ solution at the same pH and of concentration $2C_{amax}$, where C_{amax} was the highest desired concentration of aluminium. At different time intervals, two equal volumes of solutions were pipetted from each compartment; the first one was studied by light scattering and the concentration of aluminium in the second volume, measured by atomic absorption, allowed us to determine the aluminium content in the polymer solution. The two compartments were separated by an ultrafiltration Millipore membrane for molecular weight $< 10^5$. On each side of the membrane, slow magnetic stirring ensured homogeneity.

RECAP OF THE PROPERTIES OF $AlCl_3$ AND ACRYLAMIDE–ACRYLIC ACID COPOLYMERS IN AQUEOUS SOLUTIONS

Aluminium chloride ($AlCl_3$)

The $AlCl_3$ solutions contain mononuclear ions Al^{3+}, $Al(OH)^{2+}$, $Al(OH)_2^+$ and $Al(OH)_4^-$, polynuclear ions $Al_2(OH)_2^{4+}$ and $Al_{13}(OH)_p^{(39-p)+}$ and non-ionic species $Al(OH)_3$, their amounts depending on the neutralization ratio R according to six equilibrium laws of the type:

$$[Al_i(OH)_p^{(3i-p)+}] = \frac{[Al^{3+}]K_{i,p}f_{1,0}}{f_{i,p}[H^+]^i} \qquad (1)$$

where $f_{i,p}$ is the activity coefficient of $Al_i(OH)_p^{(3i-p)+}$, which can be obtained from the Debye–Huckel expression[2-4]. The solubility of Al^{3+} ions is limited by[17]:

$$[Al^{3+}][OH^-]^3 < K_{sp} \qquad (2)$$

Moreover, the polynuclear ions with degree of association 13 are metastable species, as shown by Turner[18] and confirmed by our recent n.m.r. investigations[1]. They are progressively transformed into non-ionic $Al(OH)_3$ species and a kinetic expression should be added to the previous set of relations. Nevertheless, we will neglect this phenomenon, since we have generally used freshly prepared solutions (ageing time < 8 days).

By using a set of $K_{i,p}$ and $f_{i,p}$ values given by Bottero *et al.*[4] (for $AlCl_3$ solutions aged 15 days and of concentration higher than 10^{-3} mol l^{-1}), we have calculated the composition of $AlCl_3$ solution at 10^{-3} mol l^{-1} (27 ppm) as a function of R (see *Figure 2*). For lower concentrations, we have assumed that ionic strength does not change with R and introduced values of $f_{i,p}$ calculated for an average ionic strength by the Debye–Huckel expression; the results are given in *Figure 3* for $C_a = 1.9 \times 10^{-4}$ mol l^{-1} (5 ppm). One observes that the percentage of polynuclear ions (Al_{13}) decreases by dilution. Then, at pH 5, and for low aluminium

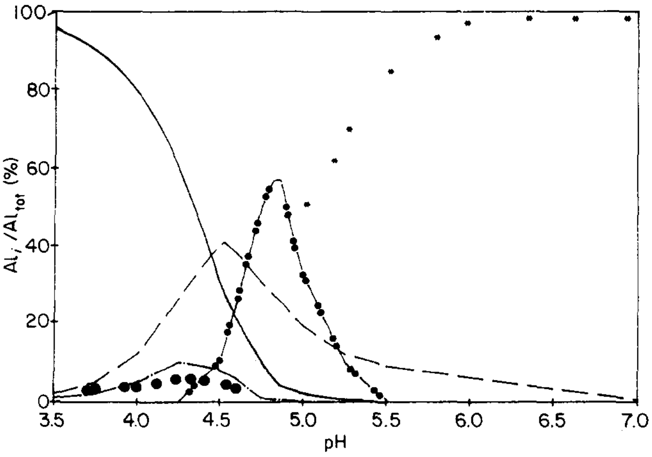

Figure 2 $AlCl_3$ solutions (27 ppm): calculated fractions of Al^{3+} (———), $Al(OH)^{2+}$ (·····), $Al(OH)_2^+$ (– – –), $Al_2(OH)_2^{4+}$ (–·–·–), $Al_{13}(OH)_{27}^{3+}$ ((–··–··–) and $Al(OH)_3$ (∗∗∗∗)

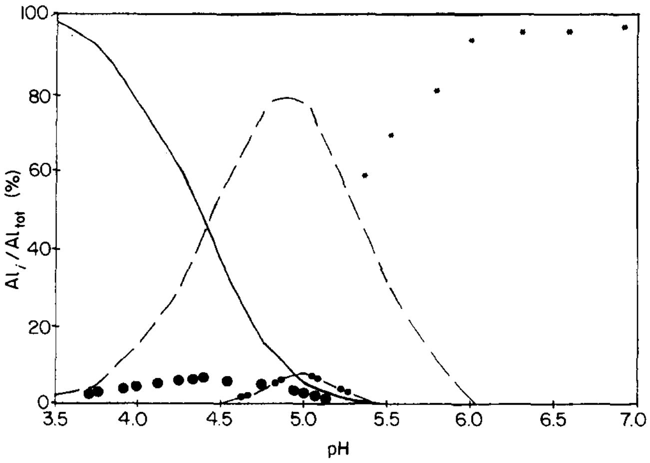

Figure 3 $AlCl_3$ solutions (5 ppm): calculated fractions of Al^{3+} (———), $Al(OH)^{2+}$ (·····), $Al(OH)_2^+$ (– – –), $Al_{13}(OH)_{27}^{3+}$ (–··–··–) and $Al(OH)_3$ (∗∗∗∗)

concentrations (< 10 ppm), only mononuclear ionic species are present, while at higher concentrations, the polynuclear ions and the non-ionic species are preponderant. At pH 7, $Al(OH)_3$ is present at more than 90% and the size of the aggregates depends on concentration and ageing time.

Acrylamide–acrylic acid copolymers

It is well known that the pK_a of polyacid can be expressed by a simple polynomial as a function of the degree of ionization[19], α:

$$pK_a = pK_{a_0} + A_1\alpha + A_2\alpha^2 + \ldots \qquad (3)$$

the values of pK_{a_0}, A_1 and A_2 depending on the acrylic acid content for the copolymers under investigation, as previously studied[20,21] (see *Table 1*). At each pH, the concentration of ionized carboxylate groups, COO^-, must obey the classical law:

$$pK_a = [COO^-][H^+]/(C_{ip} - [COO^-]) \qquad (4)$$

where C_{ip} is the molar concentration of carboxylic groups.

Aluminium–polymer interactions

In a first approximation, we have assumed a uniform distribution of the charges in the solution, neglecting the polyelectrolyte effects. Among the different possible electrostatic interactions between the polymer and the aluminium species, one can consider in a first approximation that the most important should correspond to the two following equilibria[1]:

$$Al^{3+} + 3COO^- \rightleftharpoons COO_3Al \qquad K_i \qquad (5)$$

$$Al_{13}^{3+} + 3COO^- \rightleftharpoons COO_3Al_{13} \qquad K_0 \qquad (6)$$

Starting from this assumption, we have been able to calculate the concentration of the different ionic ($Al_i(OH)_p^{(3i-p)+}$ and COO^-) and non-ionic ($Al(OH)_3$, COOH, $(COO)_3Al$ and $(COO)_3Al_{13}$) species in mixed polymer–$AlCl_3$ solutions as a function of pH and composition. This model gives a good account of n.m.r. results[1] with the values of the different equilibrium constants reported in *Table 2*. It predicts the pH ranges where the interactions will be maximum, corresponding to maxima in the concentrations of $(COO)_3Al$ and $(COO)_3Al_{13}$ (see Figure 13 of ref. 1): 4.3 and 4.8 respectively.

For the present study, the problem is the stability of the polymer when these species are formed by fixation of Al ions on the carboxylate groups. It has been shown that, in highly charged polyelectrolyte solutions in the presence of divalent cations, phase separation occurs when a given fraction of charged groups are neutralized by binding of these ions between neighbouring sites. Polymer precipitation is then observed for a molar concentration of cations of the same order of magnitude as the molar concentration of charged groups. This is the case, for instance, with polyphosphates or sodium polyacrylate[22–25]. In the simplest picture, such polyelectrolytes are considered as copolymers made up of ionized units of good solubility in water and un-ionized units of poor solubility[22]. The case of acrylamide–acrylic acid copolymer is more complex since the distance between charged groups is higher and varies with τ, and the role played by the acrylamide units cannot be neglected. However, the works of Truong *et al.*[20,26] have shown that

Table 1 Values of the parameters of relation (3)

	τ (%)	pK_{a0}	A_1	A_2
AD10	1.5	4.75	0.001	0.4
AD17	7	4.82	0.003	0.495
AD27	17	5.04	0.364	0.513
AD37	27	5.26	0.67	0.45

Table 2 Equilibrium constants

$AlCl_3$	$AlCl_3$–polymer
$K_{1,1} = 10^{-5.02}$	
$K_{1,2} = 10^{-8.72}$	
$K_{1,3} = 10^{-10.24}$	$K_i = 10^{14}$
$K_{1,4} = 10^{-42}$	
$K_{2,2} = 10^{-6.27}$	$K_0 = 10^{16}$
$K_{13,27} = 10^{-127}$	
$K_{sp} = 1.25 \times 10^{-32}$	

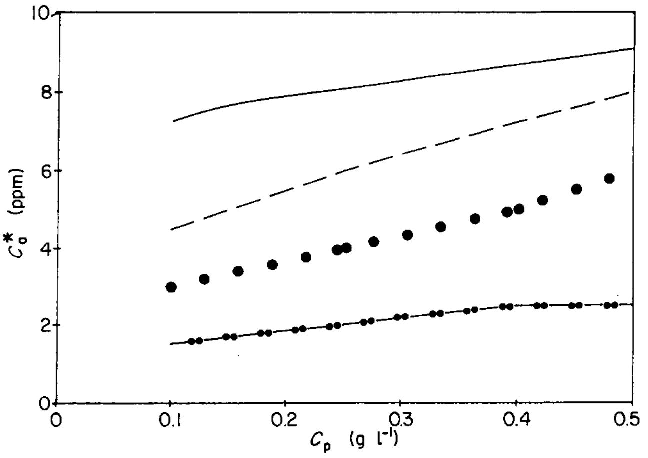

Figure 4 Variations of C_a^* as a function of polymer concentration at pH 7: AD10 (———), AD17 (–··–··–), AD27 (·····) and AD37 (– – –)

these polymers behave towards calcium as previously described if the polymer concentration range is higher than C_p^* (the critical concentration corresponding to the overlapping of the macromolecular chains), when intermolecular bridges can be created by ionic fixation (C_p^* decreasing with increasing τ), although the fraction of bound calcium ions is not very high.

With trivalent Al ions, which interact much more strongly with carboxylate groups, as clearly shown by ^{27}Al n.m.r. experiments[1], phase separation is expected for low concentration of Al in the pH ranges where these species are present. On the other hand, the high valency of these ions and their great size in the case of Al_{13}^{7+} could lead to gelation. From these considerations and taking into account the results of our calculations, we could expect the following general features for the behaviour of acrylamide–acrylic acid in the presence of aluminium:

(a) no interaction with unhydrolysed polymer, since only electrostatic interactions are considered in the model, and

(b) with hydrolysed samples, the instability maximum should be observed for the pH ranges, generally around 5, where trivalent ions are preponderant and polymer ionization high enough, while no interaction is expected at pH = 7.

RESULTS AND DISCUSSION

The concentration ranges were $0 < C_a < 20$ ppm for Al and $0 < C_p < 1000$ ppm for polymer, pH ranging between 4 and 7.

Turbidity measurements

In the range of Al concentrations investigated, the aqueous solutions of $AlCl_3$ do not present detectable turbidity even at the pH where C_a exceeds the solubility limit. For the mixed polymer–$AlCl_3$ solutions, these measurements allow us to determine the limits of compositions above which phase separation occurs. The turbidity increase can be due either to the precipitation of a polymer–aluminium complex or to the influence of the polymer on the aggregation state of the insoluble species of Al.

Unhydrolysed polyacrylamide (PAM–NH). The degree of hydrolysis of this polymer is 0.3%, a value much lower than that of the other samples. It is the reason why we will call it 'unhydrolysed', although it is slightly polyelectrolytic.

No turbidity of solutions has been detected in the concentration ranges investigated. This observation shows that even if some non-ionic interactions between aluminium species and polyacrylamide take place (particularly at pH 7), they never lead to phase separation.

Copolymer of low acrylate content (AD10). The sample AD10 of low content of acrylic acid has a particular behaviour since gelation phenomenon can be observed.

At pH 7, the turbidity of the solutions increases for aluminium concentrations higher than C_a^*, this limit increasing slightly with polymer content, as shown in *Figure 4*. This phase separation, which will be analysed later, cannot be predicted by our electrostatic interaction model. However, the stability of unhydrolysed polyacrylamide under the same conditions seems to indicate that the presence of charges on AD10 is at least partially responsible for such behaviour.

The most interesting diagram (represented in *Figure 5*) has been observed at pH 5. In this diagram, one can distinguish three distinct domains:

(a) There is a domain A of transparent solutions for Al concentrations below C_a^* with $C_a^* = 7C_{ip}$ (the two concentrations being expressed in mol l^{-1}).

(b) There is a domain B of transparent physical gels for $C_p > 200$ ppm and $7C_{ip} < C_a < 10C_{ip}$. The elastic properties of these gels have been confirmed by measurements of their elasticity modulus and this study will be reported elsewhere. This limit of polymer concentration is very near the critical concentration of C_p^* corresponding to the overlapping of the macromolecular chains[27]:

$$C_p^* = M_w/kNR_g^3 \qquad (7)$$

where R_g is the radius of gyration (2150 Å) and N is the Avogadro number. If $k = 4\pi/3$, one finds $C_p^* = 250$ ppm for AD10.

At this pH and inside the above limits of Al concentration, the calculation shows that the polynuclear ions are preponderant, their percentage being higher than 50% in the pure Al solution. This appears clearly in *Figure 6*, which shows the variation of Al^{3+} and Al_{13}^{7+} contents as a function of the total Al concentration, for

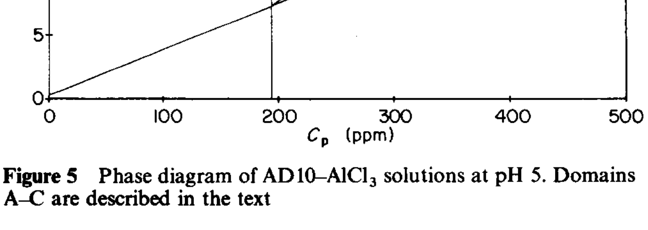

Figure 5 Phase diagram of AD10–$AlCl_3$ solutions at pH 5. Domains A–C are described in the text

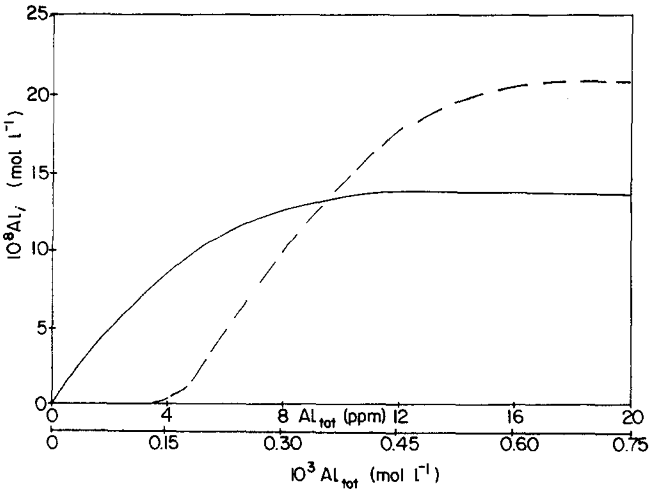

Figure 6 AlCl$_3$ solutions at pH 5: calculated concentrations of Al^{3+} (———) and Al$_{13}^{7+}$ (– – –)

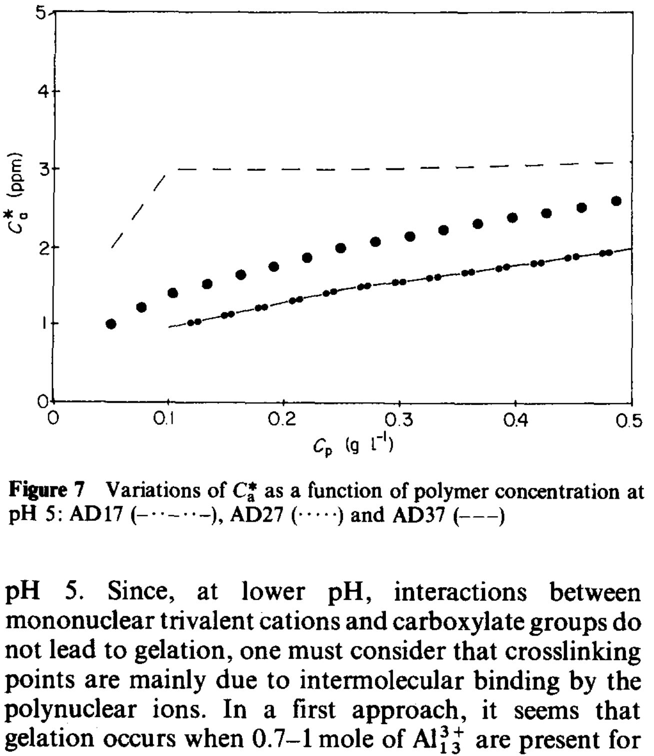

Figure 7 Variations of C_a^* as a function of polymer concentration at pH 5: AD17 (–··–··–), AD27 (·····) and AD37 (– – –)

pH 5. Since, at lower pH, interactions between mononuclear trivalent cations and carboxylate groups do not lead to gelation, one must consider that crosslinking points are mainly due to intermolecular binding by the polynuclear ions. In a first approach, it seems that gelation occurs when 0.7–1 mole of Al$_{13}^{7+}$ are present for each three carboxylate groups.

(c) There is a domain C where phase separation can be observed with formation of microgels for low polymer concentration or dense aggregates at higher C_p.

The pH range of gelation is very narrow and at pH 4 and 6 only phase separations are observed. At acid pH, the stability is higher due to the decrease in the degree of ionization of carboxylate groups and C_a^* increases by decreasing pH. At pH 6 also, turbidity occurs for values of C_a^* higher than that observed at pH 5, owing to the disappearance of charged Al species and its origin is as difficult to understand as at pH 7.

Copolymers of acrylate content between 7 and 27%. In the whole ranges of pH and composition investigated, gelation has never been observed with copolymers of acrylate content higher than 7%.

In *Figure 4*, we have reported the values of C_a^* as a function of C_p for AD10, AD17, AD27 and AD37, obtained from turbidity measurements at pH 7. The polymer that seems to be the least stable is AD17 and in the four cases C_a^* is slightly increasing with C_p. Although at this pH no electrostatic interactions are expected from the calculation of the distribution of the different Al species, the influence of the charged groups of the polymer on the turbidity of the system is clearly confirmed.

As shown in *Figures 7* and *8*, the values of C_a^* are significantly lower at pH 5 than at pH 7, but their variations with τ and C_p follow the same empirical laws. At such a pH, polymer precipitation is expected from a model of electrostatic interactions, since trivalent ionic Al species are always present. We have calculated, from our model, the percentage of carboxylate groups neutralized by the binding of these ions, $(Al(COO)_3/C_{ip})^*$, for the experimental values of C_a^* found at different values of τ and C_p (at the beginning of the phase separation). Let us recall that this model of electrostatic interactions neglects the fixation of cations of lower charge and does not take into account the inhomogeneity of the distribution of the carboxylate groups in the solution. This second approximation is incorrect for polymer concentrations lower than C_p^* and good agreement with n.m.r. experiments has been obtained for $C_p > C_p^*$ and for high values of C_a. The values of $(Al(COO)_3/C_{ip})^*$ calculated with this model are reported in *Figures 9* and *10*. *Figure 9* shows that $(Al(COO)_3/C_{ip})^*$ decreases with C_p for AD37

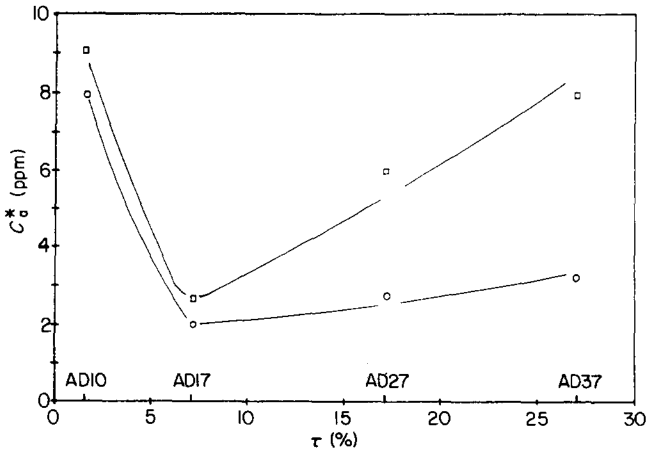

Figure 8 Variations of C_a^* as a function of degree of hydrolysis for C_p = 500 ppm at pH 5 (○) and pH 7 (□)

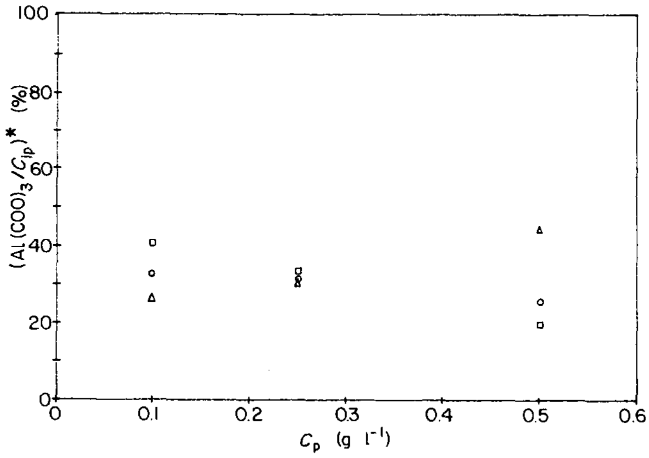

Figure 9 Calculated fractions of 'neutralized' sites as a function of polymer concentration at pH 5 and for the beginning of phase separation: AD17 (△), AD27 (○) and AD37 (□)

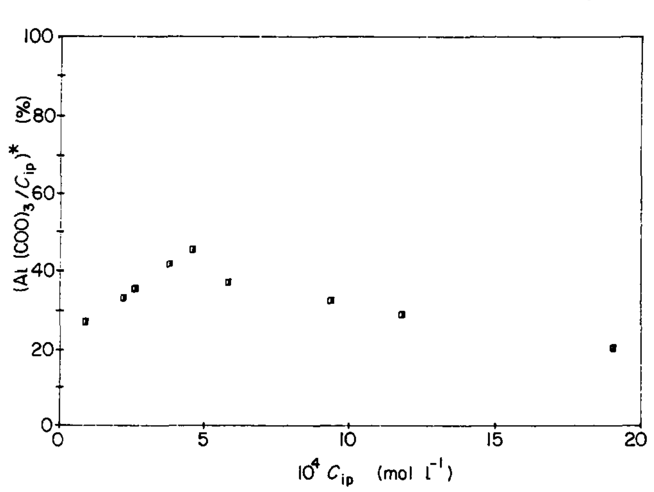

Figure 10 Calculated fractions of 'neutralized' sites as a function of molar concentration of carboxylate groups at pH 5 and for the beginning of phase separation

or AD27 and increases for AD17. The plot of the same values as a function of C_{ip} in *Figure 10* leads to a single curve, with a maximum for $C_{ip}^+ = 5 \times 10^{-4}$ mol l^{-1}. From relation (7), C_p^* is a decreasing function of τ since the presence of charges along the chain leads to a higher expansion of the coil.

The point located at the bottom of the curve of *Figure 10* corresponds to AD17 at 500 ppm, a concentration higher than but of the same order of magnitude as C_p^* for this polymer. If our model only fails for $C_p < C_p^*$, the values of $(Al(COO)_3/C_{ip})^*$ at the right of the maximum must be approximately correct: this is the case for AD37 in the whole investigated range of C_p and for AD27 if $C_p > 250$ ppm. It then appears that the neutralization ratio of carboxylate groups at the phase separation is low, between 20 and 35%, and decreases with concentration. Such a variation is not in agreement with the model of Strauss[22], which predicts a simple stoichiometry. The low value of $(Al(COO)_3/C_{ip})^*$ and the concentration dependence suggest at first the formation of aggregates by intermolecular bridges. One can also think that the binding of Al ions does not obey a random law but that the polymer chains or aggregates that have been already partially neutralized bind preferentially to other cations; this could explain the very progressive precipitation. The calculation could take into account such phenomena. For the range of low polymer concentration, $C_p < C_p^*$, one can understand that our simple model underestimates the values of $(Al(COO)_3/C_{ip})^*$, since the local concentrations of COO^- and Al ions inside the macromolecular coil are higher than the average concentration. Moreover the absence of gelation shows that, even if intermolecular bridging occurs, the cation fixation (intra- or intermolecular) leads to a high deswelling of the coils, hindering crosslinking in the whole solution.

Phase titrations

Potentiometric titration of supernatant phase. We have determined by potentiometric titration of the supernatant phase the percentage of polymer AD27 that precipitates as a function of pH for $C_p = 500$ ppm and $C_a = 5$ ppm.

In *Figure 11*, one can see that the fraction of precipitated polymer is higher than 20% for a pH range between 4 and 5, and reaches a maximum for pH 4.9 at 70%. For the pH range near neutrality, all of the polymer remains in solution, according to the turbidity results, which show that C_a^* is near 7 ppm.

In contrast to the n.m.r. results (when the Al concentration was 27 ppm), we had only one maximum because at $C_a = 5$ ppm, the amount of Al_{13} is less than 10% (see *Figures 2* and *3*) and the main interaction is $Al^{3+} + 3COO^-$.

The fractions of precipitated polymer are compared in *Figure 11* with the concentration values of the species COO_3Al. The two curves have the same dependence on pH; this shows that for low Al concentrations, our model is in qualitatively good agreement with the experimental observations, by considering that the formation of COO_3Al species is responsible for polymer precipitation.

Viscosity measurements realized on the same samples confirm this pH dependence of the stability of AD27 solutions (see *Figure 11*, where we have reported the variation of the ratio η/η_0 as a function of pH, η_0 being the viscosity of free Al solutions at the same pH; η and η_0 are measured at the Newtonian plateau).

Titration of the precipitated phase. We have studied here a range of higher aluminium concentrations where the ionic polynuclear and the non-ionic species appear at lower pH and where the size of $Al(OH)_3$ aggregates is expected to be higher.

(i) *Unhydrolysed polyacrylamide.* No precipitated phase was obtained for aluminium concentrations up to 40 ppm, in agreement with the turbidimetric observations.

(ii) *Acrylamide–acrylic acid copolymer of* $\tau > 7\%$. All these experiments were performed for $C_a = 20$ ppm, above C_a^*, at pH 5 and 7 and for $C_p = 500$ ppm.

In *Table 3*, we have reported the values of the fraction of precipitated polymer and the fraction of polymer in the precipitated phase. At pH 7, the presence of polymer in the solid phase shows that the turbidity is due to polymer precipitation. At this pH, the fraction of precipitated polymer is lower than at pH 5 but for the two pH values one observes that the polymer samples of $\tau = 7$ and 17% are less stable than samples of lower or higher τ, as already shown by turbidimetry. On the other hand, the

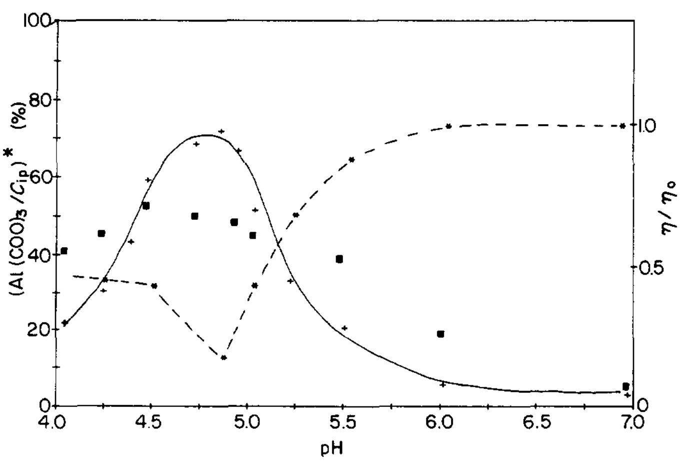

Figure 11 System AD27–$AlCl_3$ ($C_p = 500$ ppm, $C_a = 5$ ppm) at different pH values. Experimental results: fraction of precipitated polymer determined by potentiometric titration (+) and viscosity ratio η/η_0 (see text) (*). Calculated values: the fraction of 'neutralized' sites (■)

Table 3 Titration of the precipitated phase

pH		Fraction of precipitated polymer (%)	Polymer fraction in precipitated phase (%)	Weight of precipitated phase (mg)	
				Expt.	Theor.
5	AD17	18	66	18.7	1.4–3.0
	AD27	12	56	19	3.2–6.9
	AD37	9	48	19	5.4–11.6
7	AD17	5	33	21	–
	AD27	6.3	32	25	–
	AD37	1	13	12	–

precipitated phase contains a fraction of aluminium that increases with increasing τ. In the penultimate column of *Table 3*, we give the difference between the total weight of the coacervate and the weight of polymer in it. This difference, Δx_a, must be attributed to different aluminium species present in the coacervate.

At pH 5, Δx_a is nearly constant for the three samples and approximately equal to 19 mg. In fact only 9 mg of Al have been introduced in the solution and the discrepancy between the two values can be explained by considering that Al is present as $Al_i(OH)_p$, with $p=2i$. From our model, only Al^{3+} and $Al_{13}(OH)_{27}$ are expected to be bound on polymer and we have previously determined the total concentration of bound carboxylate groups $Al(COO)_3$ (ref. 1). We have deduced the values of Δx_a that would correspond to the fixation of each of the species. The obtained values reported in the last column of *Table 3* are much lower than the experimental values. Moreover, the calculated values of Δx_a increase with increasing τ. Since our model is in good agreement with our previous n.m.r. results, which are only relative to the fixation of the ionic species, we can conclude that electrostatic interactions are not the main force in polymer precipitation. The 'non-ionic' species $Al(OH)_3$, which represents approximately 50% of Al at pH 5, probably also plays a role.

At pH 7, our model does not predict any interaction between polymer and $Al(OH)_3$. The values of Δx_a are, however, consistent with the presence of this species in the coacervate. This result definitely confirms the existence of an interaction with the polymer. Although hydrogen bonds are expected between amide groups and the OH functions of $Al(OH)_3$, the strong dependence of C_a^* and Δx_a on the polymer charge as well as the absence of phase separation in unhydrolysed polyacrylamide suggest that some residual charges remain on the $Al(OH)_3$ aggregates in insufficiently aged solutions. The size of the $Al(OH)_3$ aggregates must also play a role, the formation of intermolecular bridging being favoured at high aluminium concentration. This could explain why no precipitation has been observed with AD27 at $C_a = 5$ ppm, at pH 7.

We should like to remark that there is a contradiction between the results obtained by the two methods (titration of supernatant or that of coacervate) for AD27 at pH 5. Indeed, the fraction of precipitated polymer found by the first method for $C_a = 5$ ppm (50%) is surprisingly higher than that determined by the second method for $C_a = 20$ ppm (12%) in contradiction to theoretical predictions and turbidimetry results. Two explanations can be proposed:

(a) The porosity of the filters used in the second method is higher and the small aggregates are not separated.

(b) If sample AD27 is rather inhomogeneous in degree of hydrolysis, the less hydrolysed fraction is expected preferentially to remain in solution. Then the method based on a potentiometric titration must lead to an underestimate of the soluble fraction and consequently an overestimate of the precipitated fraction. Truong *et al.*[13] have shown that τ is between 15 and 25% for AD27.

Viscometry

Unhydrolysed polyacrylamide (PAM–NH). As the viscosity of the polymer solutions is only 1.5 to 2 times that of water, a capillary viscometer has been used to determine the influence of the presence of aluminium in the solution. At pH = 5, as at pH = 7, we note a decrease of the reduced viscosity (*Figure 12*). This result shows that PAM–NH interacts with aluminium, although no phase separation has been observed. We recall, first, that PAM–NH is slightly charged ($\tau = 0.3\%$) and its polyelectrolyte character is confirmed by the difference of the η_{red} values at pH 5 and 7, for free aluminium solutions. Then the viscosity decrease with Al content at pH 5 must be partially due to electrostatic screening by ionic Al species. At pH 7, the adsorption of the chain on the $Al(OH)_3$ aggregates can probably be considered as the main origin of the loss of viscosity.

Copolymer of low acrylate content (AD10). As previously described, at pH = 5 the AD10 sample has a particular behaviour due to the gelation phenomenon. Thus in the domain B of the phase diagram (*Figure 5*), an increase in the viscosity of the polymer solution can be observed, while for all of the other samples and for the other range of pH, we note a reduction in the viscosity values in the presence of the aluminium species. We compare in *Figures 13* and *14*, the evolutions of the η vs. γ curves by increasing Al content for AD10 and AD27, at pH 5 and for the same polymer concentration.

Copolymers of acrylate content between 7 and 27%. The viscosity of AD copolymer–$AlCl_3$ solutions has been measured at pH 5 and 7, for $100 < C_p < 500$ ppm and for $0 < C_a < 20$ ppm. Some variations of η measured at the

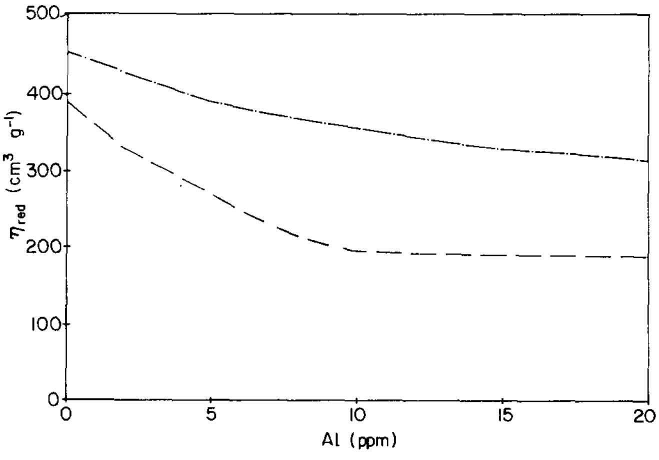

Figure 12 Variations of reduced viscosity of unhydrolysed polyacrylamide (PAM–NH) (250 ppm) with Al concentration at pH 5 (– – –) and pH 7 (–·–·–)

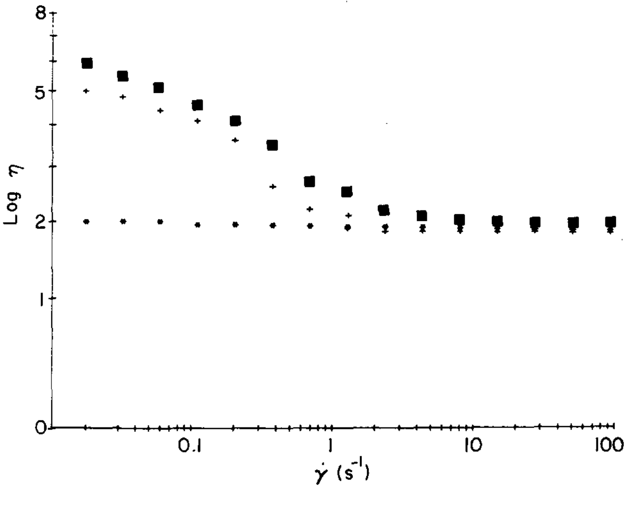

Figure 13 Variations of AD10 solution (550 ppm) viscosity (measured in centipoise) vs. shear rate at pH 5 for different aluminium concentrations: 0 ppm (*), 15 ppm (+) and 20 ppm (■)

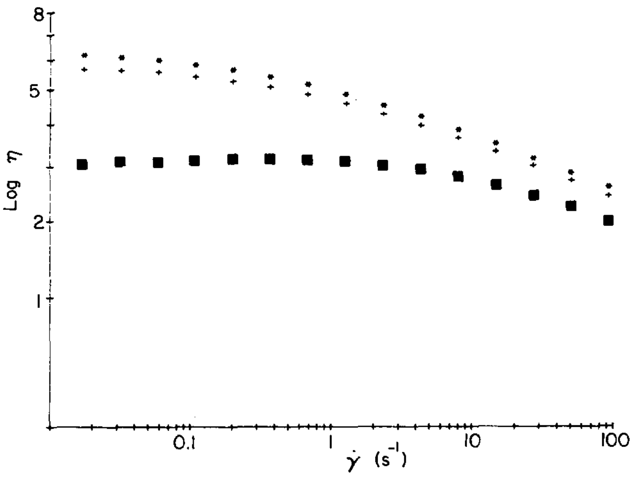

Figure 14 Variations of AD27 solution (500 ppm) viscosity (measured in centipoise) vs. shear rate at pH 5 for different aluminium concentrations: 0 ppm (*), 5 ppm (+) and 10 ppm (■)

Newtonian plateau for AD17 and AD27 are represented in *Figures 15* and *16* respectively.

At pH = 5 as well as at pH = 7, the viscosity of the polymer solutions decreases in the presence of a very low number of aluminium species. This decrease is observed even for $C_a < C_a^*$, when the solution is still transparent and for all values of C_p. The variation of η_{red} was found to be faster for the lower polymer concentrations. So one can expect that the reduction of viscosity is due to two phenomena:

(i) *Deswelling of the coils for* $C_a < C_a^*$. At pH = 5, we can consider that it is due to the screening of electrostatic interactions and to 'site neutralization' by the trivalent mononuclear ions. At low C_p, this corresponds to a coil–globule transition, while for $C_p > C_p^*$, the intermolecular association of the deswollen coils must play an additive role on the hydrodynamic properties.

At pH = 7, when practically all of the Al is converted into $Al(OH)_3$, one can assume that the polymer is adsorbed on the $Al(OH)_3$ species through hydrogen bonds, this adsorption probably being favoured by the presence of charges on the polymer and $Al(OH)_3$ aggregates.

(ii) *Phase separation for* $C_a > C_a^*$. This phenomenon has been described above, and leads to precipitation of the polymer and then to decrease of the viscosity.

Light scattering

The light scattering measurements are always made in the presence of NaCl (0.1 M). The values of C_a^* are slightly higher than those found in free NaCl solutions. For instance $C_a^* > 5$ ppm for AD27 (250 ppm) while $C_a^* = 2$ ppm in the absence of NaCl. It is known that the stability of these copolymers towards divalent cations (Ca^{2+}) increases by increasing the amount of salt of monovalent metals[26]. This is due to competition between the interactions of the different ions with the polymer.

We have limited our investigations to the cases where precipitation occurs.

We will give here one example of light scattering results, which for $C_p \neq C_p^*$ confirm the mechanism of aggregation and deswelling. In *Figure 17*, we give a kind of Zimm plot where on the abscissa we plot $(\sin^2\theta/2 + C_a)$, C_p being constant. It can be seen that the extrapolation to $\theta = 0$ decreases on increasing C_a, this behaviour corresponding to an increase of molecular weight. Moreover, the radius of gyration passes through a

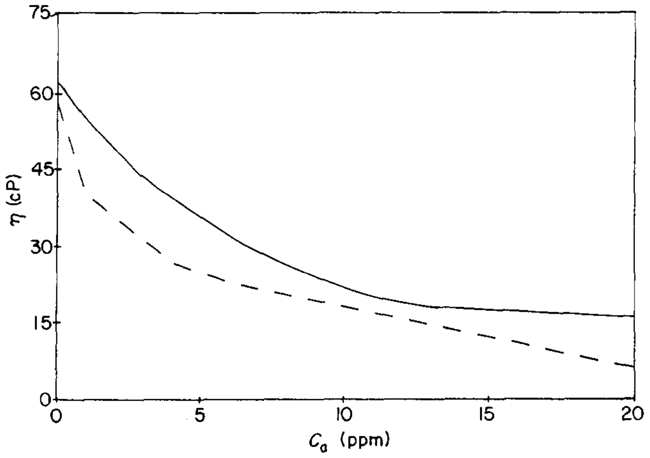

Figure 15 Variations of AD17 solution (500 ppm) viscosity (at the Newtonian plateau) vs. aluminium concentration: pH 5 (– – –) and pH 7 (———)

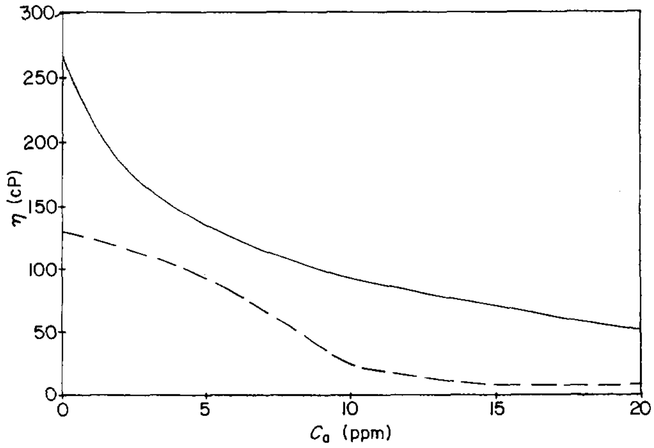

Figure 16 Variations of AD27 solution (500 ppm) viscosity (at the Newtonian plateau) vs. aluminium concentration: pH 5 (– – –) and pH 7 (———)

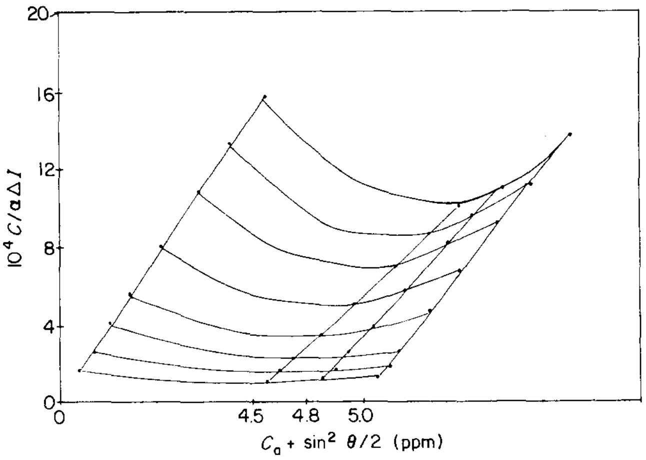

Figure 17 Light scattering of AD27 solutions (250 ppm) at pH 5 for different aluminium contents (see text)

maximum: in a first step, there is aggregation of partially deswollen coils and the resulting dimensions become higher; however, in the same range of C_a the decrease in viscosity indicates that the ratio R_g^3/M is a decreasing function of C_a. In a second step, the deswelling becomes more important near C_a and, although the aggregation number increases, the dimensions are lower.

CONCLUSIONS

This work shows that the stability of acrylamide–acrylic acid copolymer is very poor in aqueous solutions that contain $AlCl_3$.

A maximum of instability was expected at pH 5 from a simple model of electrostatic interactions in which phase separation is attributed only to the neutralization of polymer charge by the different Al ionic species. Our results confirm this prediction but also reveal that one cannot neglect interactions with non-ionic species ($Al(OH)_3$).

For a very low degree of hydrolysis (0.3%), no phase separation occurs although some viscosity decrease is observed.

In very narrow ranges of τ and pH (around 5), a gelation phenomenon appears if 0.7–1 mole of polynuclear ion $Al_{13}(OH)_{27}^{3+}$ is present for each three carboxylate groups. This phenomenon can only occur if τ is high enough to allow electrostatic interactions and low enough to favour strongly intermolecular bridging with respect to intramolecular fixation. This has been observed, in this work, for $\tau = 1.5\%$, but we are not able to give an upper limit for τ, which is also expected to depend on molecular weight. In this case the solution viscosity increases.

For $\tau > 7\%$, phase separation always occurs for aluminium contents that never exceed 10 ppm (if $C_p < 500$ ppm), the critical concentration C_a^* being a minimum at pH 5. For $C_a < C_a^*$, the viscosity is a decreasing function of C_a even if aggregates are formed by intermolecular bridging. At pH 5, these phenomena mainly originate from electrostatic interactions but non-ionic interactions preponderant at pH 7 must be taken into account.

From a theoretical viewpoint, our first interaction model, which has previously given a good account for ^{27}Al n.m.r. investigations, must be improved by considering the inhomogeneity in the repartition of the ions in a dilute polyelectrolyte solution and taking into account non-ionic interactions.

ACKNOWLEDGEMENTS

This work has benefited from grants from Institute Français du Pétrole and we thank Dr J. Lecourtier and Dr G. Chauveteau for fruitful discussions. The authors are indebted to Dr H. Kheradmand for the preparation of the PAM–NH sample and to Dr D. Sarazin for his help in light scattering experiments.

REFERENCES

1 Rabhari, R. and François, J. *Polymer* 1988, **29**, 845
2 Bottero, J. Y., Cases, J. M. and Fiessinger, F. *J. Phys. Chem.* 1980, **84**, 2933
3 Bottero, J. Y., Marchal, J. P., Cases, J. M. and Poirier, J. E. *Bull. Soc. Chim. Fr.* 1982, **11–12**, I-439
4 Bottero, J. Y., Tchoubar, D., Cases, J. M. and Fiessinger, F. *J. Phys. Chem.* 1982, **86**, 3667
5 Akitt, J. W., Greenwood, W. N. and Khandelwal, B. L. *J. Chem. Soc.* 1972, 604
6 Akitt, J. W., Greenwood, W. N. and Lester, S. D. *J. Chem. Soc.* 1972, 803
7 Akitt, J. W. and Farthing, A. *J. Magn. Reson.* 1978, **32**, 345
8 Mungan, N. *Soc. Petroleum Eng. J.* 1972, Dec., 469
9 Nouri, H. H. and Root, P. J. Paper SPE 3523 Presented at the SPE 46th Annual Meeting, New Orleans, 1971
10 Martin, F. D. and Sherwood, N. S. Paper SPE 5339 Presented at the SPE 50th Annual Meeting, Denver, 1975
11 Muller, G., Lainé, J. P. and Fenyo, J. C. *J. Polym. Sci.* 1979, **17**, 659
12 Boutin, J. and Contat, S., French Patent 249217 issued to Rhône-Poulenc Ind., 1980
13 Truong, N. D., Galin, J. C., François, J. and Pham, Q. T. *Polymer* 1986, **27**, 467
14 Gramain, P. and Libeyre, R. *J. Appl. Polym. Sci.* 1970, **14**, 383
15 Libeyre, R., Sarazin, D. and François, *J. Polym. Bull. (Berlin)* 1981, **4**, 53
16 Schwartz, T. and François, J. *Makromol. Chem.* 1981, **182**, 2757
17 Bolt, G. H., 'Soil Chemistry', Elsevier, New York, 1978, Vol. 1, Ch. 6
18 Turner, R. C. *Can. J. Chem.* 1976, **54**, 1528
19 Mandel, M. *Eur. Polym. J.* 1970, **6**, 807
20 Truong, N. D., Thesis, Strasbourg, 1984
21 Lainé, J. P., These de 3ème cycle, Rouen, 1977
22 Armstrong, R. W. and Strauss, U. P. 'Encyclopedia of Polymer Science and Technology', Interscience, New York, 1969, Vol. 10
23 Strauss, U. P. and Siegel, A. *J. Phys. Chem.* 1963, **67**, 2683
24 Ikegami, A. and Imai, N. *J. Polym. Sci.* 1962, **56**, 133
25 Michaeli, J. *J. Polym. Sci.* 1960, **48**, 291
26 Truong, N. D. and François, J. *Collect. Colloq. Semin.* 1984, **42**, 251
27 de Gennes, P. G. 'Scaling Concepts in Polymer Physics', Cornell University Press, Ithaca, NY, 1979